International Journal of Mass Spectrometry and Ion Physics, 16 (1975) 167–189

FLOWING AFTERGLOW STUDIES AT YORK UNIVERSITY

HAROLD I. SCHIFF AND DIETHARD K. BOHME

Department of Chemistry and Centre for Research in Experimental Space Science, York University, Downsview, Ontario (Canada)

(Received 17 July 1974)

ABSTRACT

The flowing afterglow system at York University is being used to obtain both kinetic and thermodynamic data for ion–molecule reactions. The kinetic measurements have been directed mainly to testing current reaction rate theories. The ADO theory appears to predict results which agree within 40 % with experiments for proton transfer reactions to neutral molecules which have permanent dipole moments from zero to 2.98 D. The classical theories predict much higher values than those observed for other reactions, such as those involving CH_3^+ transfer, for which "ab initio" calculations predict the presence of energy barriers in the potential surface. These reactions can be represented as having activation energies, E_a ca. >5 kcal mole^{-1}. Exothermic reactions of C^-, C_2^- and C_2H^- with H_2, O_2, CO, CO_2, H_2O, CH_4 and C_2H_2 were also found to be very slow, due to chemical effects associated with multiple bond rearrangement or close range electrostatic interaction. Rate constants have also been measured for reactions believed to be important in the synthesis of polyatomic molecules observed in interstellar space, examples of which are the formation and loss processes suggested for HCN.

Equilibrium constant measurements have been made by two independent methods: the ratio of rate constants measured in the forward and reverse direction, and the ratio of the concentration of products to reactants measured at equilibrium. Such measurements for proton transfer reactions to neutral molecules, when combined with measured or calculated values of $\Delta S°$ lead to a table of proton affinity differences of neutral molecules. The same principle applied to negative ions has led to the determination of proton affinities of negative ions, acidities of Bronsted acids, electron affinities and bond dissociation energies of neutral molecules.

INTRODUCTION

The flowing afterglow (FAG) system, originally developed [1] in the NOAA laboratories at Boulder, Colorado, has proven to be one of the most powerful techniques for obtaining rate constants of ion–molecule reactions at thermal energies. The FAG system at York University has been used to measure rate constants of reactions selected mainly to test current reaction rate theories which assume Boltzmann distributions. However, we have also found the technique to be equally potent in obtaining thermodynamic data for ion–molecule reactions from which it is possible to derive values for such fundamental properties as heats of formation of ions, proton affinities of neutral molecules and negative ions gas phase acidities), electron affinities and bond-dissociation energies of molecules. These studies have become the major focus of the work here.

RATE CONSTANT MEASUREMENTS OF ION–MOLECULE REACTIONS

The current classical theory of ion–molecule reactions yields, for the macroscopic rate constant of a reacting system having a Boltzmann distribution, the expression

$$k = \frac{2\pi q}{\mu^{\frac{1}{2}}} \left\{ \alpha^{\frac{1}{2}} + C\mu_D \left(\frac{2}{\pi kT} \right)^{\frac{1}{2}} \right\}$$

where q is the charge on the ion, μ the reduced mass, μ_D is the permanent dipole moment and α is the polarizability of the neutral molecule. C is a parameter, introduced by Su and Bowers [2], which can have values from 0 to 1 and is a measure of the extent to which the permanent dipole is oriented to the direction of the approaching ion. If either C or μ_D is zero the expression reduces to the familiar Langevin expression [3]. When C is unity the expression is identical to the locked dipole theory [4, 5] in which the dipole is considered to be oriented continuously along the line of centres. Su and Bowers [2] considered that the permanent dipole has an effective average dipole orientation (ADO) and deduced that C is a function only of $\mu/\alpha^{\frac{1}{2}}$ at a given temperautre. They have provided values of C at 300 K [6].

The theory involves a number of simplifying assumptions. The treatment is classical and assumes no dependence on the size or moment of inertia of the molecule. It is purely physical, involving only the physical parameters μ_D, α and μ. It, therefore, does not account for such chemical effects as energy or entropy of activation or the exothermicity of the overall reaction.

Proton transfer reactions should provide a good test for the theory since such chemical constraints would not be expected for the simple transfer of a proton from one molecule to another. There are other advantages to selecting

proton transfer reactions. They are generally "clean", without complications from other primary or secondary channels. Moreover a series of reactions in which the proton transfer to the same neutral molecule from a variety of proton donors XH^+ permits an assessment of the effect of exothermicity on reactions which are otherwise similar.

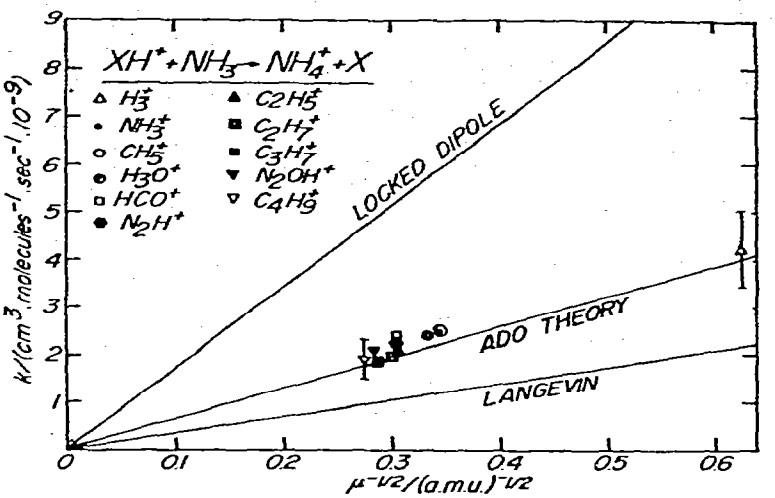

Fig. 1. A comparison of experimental rate constants at 300 K for proton transfer reactions to $NH_3(\mu_D = 1.47$ D) with predictions from classical theories.

Figure 1 illustrates the case of proton transfer from positive ions XH^+ to NH_3 [7] which has a permanent dipole moment $\mu_D = 1.47$ D. The ADO theory appears to account satisfactorily for the dependence of k on the physical parameters μ_D, μ and α and moreover to have provided a reasonable value for the parameter C. This is also seen in Fig. 2 which shows the ratio of the experimental

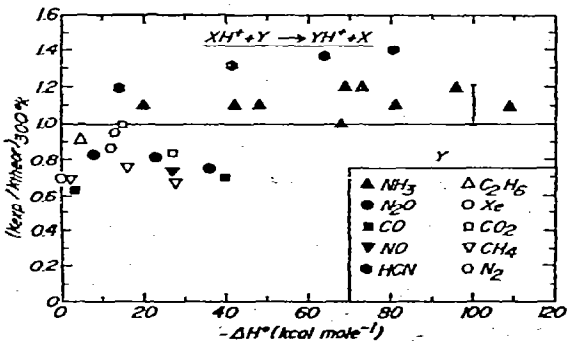

Fig. 2. A plot of the ratio of the experimental to the theoretical rate constant at 300 K as a function of the exothermicity, $-\Delta H°$, for proton transfer reactions from a variety of positive ions to molecules having small or zero values of μ_D and with NH_3 and HCN having $\mu_D = 1.47$ D and 2.98 D respectively. The ± 10 % precision of the measurements are represented by the error bar.

to the theoretical rate constants, k_{exp}/k_{theor}, for a variety of proton transfer reactions from positive ions. For those molecules with small or zero values of μ_D the ADO (or Langevin) theory predicts values which are somewhat (up to 40 %) larger than observed. For molecules having large dipole moments (NH_3 and HCN) the ADO theory predicts values which are somewhat (up to 40 %) smaller than observed. There is no obvious dependence on the moment of inertia or size of the molecule, nor on the exothermicity of the reaction. For rate constants of proton transfer reactions of the type $Y^- + HX \rightarrow X^- + HY$, the agreement with ADO theory is less satisfactory, with the ratio k_{exp}/k_{theor} spanning the range 0.4–2.2.

We have recently extended our experimental assessment of theory to quantum mechanical investigations which do not completely ignore chemical effects. Recent semi-empirical and "ab initio" calculations of potential energy surfaces have predicted the existence of energy barriers for certain ion–molecule reactions. For example, the semi-empirical calculations of Kuntz and Roach [8] indicate an energy barrier of ca. 15 kcal mole^{-1} in the entrance valley of the potential energy surface for the reaction

$$Kr^+ + H_2 \rightarrow KrH^+ + H \qquad (1)$$

Also, the "ab initio" LCAO–MO–SCF calculations of Dedieu and Veillard [9] imply an energy barrier of 3.8 kcal mole^{-1} for what is formally a methyl cation, CH_3^+, transfer reaction

$$H^- + CH_3F \rightarrow CH_4 + F^- \qquad (2)$$

One can attempt to account for such energy barriers in the traditional Arrhenius manner:

$$k_{exp} = k_{capture} \exp(-E_a/RT) \qquad (i)$$

where k_{exp} is the measured and $k_{capture}$ is the capture rate constant calculated using classical theories in the manner indicated earlier in this paper. While such an approach represents a gross oversimplification as a model for including chemical effects in ion–molecule reactions, it does represent an advance over the purely physical theory. Should there be reasons other than an energy barrier which cause the measured rate constant to be less than the capture rate constant, such as a T^{-n} dependence of the pre-exponential term, the activation energy barrier, E_a, calculated using eqn. (i) will be too large.

In the case of reaction (1) our experimental measurement [10] of a rate constant of $(2.0 \pm 0.5) \cdot 10^{-10}$ cm^3 molecule^{-1} s^{-1} corresponds to an activation energy of, at most, 1.2 kcal mole^{-1}, which does not support the large energy barrier estimated theoretically. The accord between theory and experiment is better for reaction (2). The theoretical prediction of a barrier of 3.8 kcal mole^{-1} is in remarkable (but probably fortuitous) agreement with the experimental value of 3.6 kcal mole^{-1} which can be deduced, using eqn. (i), from the measured rate

TABLE 1

RATE CONSTANTS AND ACTIVATION ENERGIES FOR EXOTHERMIC CH_3^+ TRANSFER REACTIONS FROM CH_3Cl IN THE GAS PHASE AT 296 K[a]

Anion	$-\Delta H°_{298}$ (*kcal mole*$^{-1}$)	k_{exp}[b]	k_{ADO}[c]	k_{exp}/k_{ADO}	E_a[d] (*kcal mole*$^{-1}$)
H^-	86±1	2.5[e]	8.5	0.29	0.7±0.2
NH_2^-	66.1±0.2	2.1[a]	2.4	0.88	0.1±0.2
OH^-	49±1	1.9[a]	2.4	0.79	0.1±0.2
F^-	29±8	1.8[a]	2.3	0.78	0.1±0.2
C_2H^-	62±1	0.12	2.1	0.057	1.7±0.2
CN^-	30±4(15±4)[f]	ca. <0.0004	2.0	ca. <0.0002	ca. > 5

[a] Units are · 10^{-9} cm^3 molecule^{-1} s^{-1}.
[b] Unless indicated otherwise, the accuracy is ±20 %.
[c] Calculated using the average-dipole-orientation theory [6]. The adjustable parameter, $C = 0.21$.
[d] See eqn. (i). The uncertainty in E_a reflects only the uncertainty in k_{exp}.
[e] Ref. 12. Accuracy is ±30 %.
[f] Production of isocyanomethane.

TABLE 2

RATE CONSTANTS AND ACTIVATION ENERGIES FOR CH_3^+ TRANSFER REACTIONS FROM CH_3F IN THE GAS PHASE AT 296 K[a]

Anion	$-\Delta H°_{298}$ (*kcal mole*$^{-1}$)	k_{exp}[b]	k_{ADO}[c]	k_{exp}/k_{ADO}	E_a[d] (*kcal mole*$^{-1}$)
H^-	57±8	0.015	7.6	0.0020	3.6±0.1
NH_2^-	37±9	0.017	2.3	0.0074	2.9±0.1
OH^-	20±8	0.024	2.2	0.011	2.6±0.1
C_2H^-	33±9	ca. <0.0003	2.0	ca. <0.00015	ca. >5
CN^-	1±11(−14±11)[e]	ca. <0.00	2.0	ca. <0.00015	ca. >5

[a] Units are · 10^{-9} cm^3 molecule^{-1} s^{-1}.
[b] The accuracy is ±20 %.
[c] Calculated using the average-dipole-orientation theory, [6]. The adjustable parameter $C = 0.23$.
[d] See eqn. (i). The uncertainty in E_a reflects only the uncertainty in k_{exp}.
[e] Production of isocyanomethane.

constant of $(1.5\pm0.3)\cdot10^{-11}$ cm^3 molecule^{-1} s^{-1}. The rate constant measurements summarized in Tables 1 and 2 for other CH_3^+ transfer reactions studied in this laboratory [11] suggest the presence of activation energies in other reactions of this type, especially in the reactions of CN^- with CH_3Cl and of C_2H^- with CH_3F. More decisive experimental evidence for the presence and magnitude of activation energies in reactions of this type would of course be provided by the measurement of the rate constants for these reactions at various temperatures.

A large number of reactions of this type have been studied extensively in solution where they are known as bimolecular nucleophilic displacement or S_N2 reactions. Both the rates and preferred directions of S_N2 reactions have been

observed to be sensitive to the nature of the solvent medium. The gas phase measurements described above provide the first opportunity to determine the intrinsic nucleophilic reactivity of "nude" anions and hence to assess the role of solvation in condensed phase S_N2 reactions. For example, an important question arises regarding the origin of the large activation energies, E_a ca. 15–20 kcal mole^{-1}, characteristic of reactions of anions with methyl halides in solution. To what extent do these observed activation energies reflect intrinsic properties of the chemical reaction and not, therefore, solvent effects? Our gas phase measurements suggest that several S_N2 reactions may possess large intrinsic activation energies, E_a ca. >5 kcal mole^{-1}. This, of course, implies that not all of the activation energy observed for such reactions in solution is necessarily attributable to solvent effects. The presence of intrinsic activation energies would also dictate that classical theories of capture can only hope to predict an upper limit to the rate of these reactions in the gas phase, in much the same way that the diffusion limited rate provides an upper limit in solution.

To probe further into chemical effects on the rates of ion–molecule reactions we have turned our attention to the reactions of ions for which one might anticipate the presence of steric or energetic constraints. Initially attention was focussed on the reactions of C^-, C_2^- and C_2H^- whose study was stimulated in part by the importance of the latter two ions in combustion chemistry. The ions, C_2^- and C_2H^- dominate the negative-ion spectrum of fuel-rich hydrocarbon flames [13] and are proposed as the precursors of the large unsaturated carbonaceous anions $C_xH_y^-$ ($x \geq 3$, $y \geq 0$) observed in these flames.

TABLE 3

REACTIONS OF C_2^- WITH H_2, O_2, CO, CO_2, H_2O, CH_4 AND C_2H_2 AT 298 K

$C_2^-(^2\Sigma)+H_2(^1\Sigma)$	$\rightarrow C_2H_2(^1\Sigma)+e+70^a$	A[b]	$\leq 1(-13)$[c]
	$\rightarrow C_2H^-(^1\Sigma)+H(^2S)+0$	A	
$C_2^-(^2\Sigma)+O_2(^3\Sigma)$	$\rightarrow C_2O_2(^1\Sigma)+e+?$	A	2.1(−11)
	$\rightarrow 2CO(^1\Sigma)+e+177$	A	
	$\rightarrow CO_2(^1\Sigma)+C(^3P)+e+47$	A	
	$\rightarrow C_2O^-(^2\Sigma)+O(^3P)+?$	A	
	$\rightarrow C^-(^4S)+CO_2(^1\Sigma)+77$	A	
	$\rightarrow O^-(^2P)+C_2O(^3\Sigma)+6$	A	
$C_2^-(^2\Sigma)+CO(^1\Sigma)$	$\rightarrow C_3O(^3\Sigma)+e+?$		$\leq 1(-12)$
$C_2^-(^2\Sigma)+CO_2(^1\Sigma)$	$\rightarrow C_3O_2(^1\Sigma)+e+77$	A	$\leq 5(-13)$
$C_2^-(^2\Sigma)+H_2O(^1A_1)$	$\rightarrow C_2H_2O(^1A_1)+e+81$	A	$\leq 1(-12)$
	$\rightarrow CO(^1\Sigma)+CH_2(^3\Sigma)+e+?$	A	
$C_2^-(^2\Sigma)+CH_4(^1A_1)$	$\rightarrow CH_3C{\equiv}CH(^1A)+e+62$	A	$\leq 1(-13)$
	$\rightarrow CH_2{-}C{-}CH_2(^1A)+e+46$	A	
	$/\Delta+e+39$		
	$\rightarrow C_2H^-(^1\Sigma)+CH_3(^2A_2'')+0$	A	
$C_2^-(^2\Sigma)+C_2H_2(^1\Sigma)$	$\rightarrow CH{\equiv}C{-}C{\equiv}CH(^1\Sigma)+e+76$	A	$\leq 1(-13)$

[a] Reaction exothermicity in kcal mole^{-1}. Only exothermic reactions are given.
[b] A ≡ Overall spin conservation.
[c] Measured rate constant in units of cm^3 molecule^{-1} s^{-1}. (−13) Denotes 10^{-13}.

TABLE 4

REACTIONS OF C_2H^- WITH H_2, O_2, CO, CO_2, H_2O, CH_4 AND C_2H_2 AT 298 K

$C_2H^-(^1\Sigma)+H_2(^1\Sigma)$	$\rightarrow C_2H_3+e+6$[a]		$\leq 1(-13)$[b]
$C_2H^-(^1\Sigma)+O_2(^3\Sigma)$	$\rightarrow 2CO(^1\Sigma)+H(^2S)+e+71$	A[c]	$\leq 1(-13)$
	$\rightarrow COOH^-+C(^3P)+20$	A	
	$\rightarrow H^-(^1S)+2CO(^1\Sigma)+90$	F	
	$\rightarrow OH^-(^1\Sigma)+C_2O(^3\Sigma)+13$	A	
$C_2H^-(^1\Sigma)+CO(^1\Sigma)$	$\rightarrow HC_3O(^2\Sigma)+e+?$	A	$\leq 1(-12)$
$C_2H^-(^1\Sigma)+CO_2(^1\Sigma)$	$\rightarrow HC_3O_2+e+?$		$\leq 1(-13)$
$C_2H^-(^1\Sigma)+H_2O(^1A_1)$	$\rightarrow C_2H_3O+e+18$	A	$\leq 1(-12)$
	$\rightarrow CO(^1\Sigma)+CH_3(^2A_2'')+e+6$	A	
$C_2H^-(^1\Sigma)+CH_4(^1A_1)$	$\rightarrow CH_2CH-CH_2+e+23$	A	$\leq 1(-13)$
$C_2H^-(^1\Sigma)+C_2H_2(^1\Sigma)$	$\rightarrow CH_2=CH-C\equiv C+e+?$	A	$\leq 1(-13)$

[a] Reaction exothermicity in kcal $mole^{-1}$. Only exothermic reactions are given.
[b] Measured rate constant in units of cm^3 $mole^{-1}$ s^{-1}. (−13) Denotes 10^{-13}.
[c] A ≡ Overall spin conservation; F ≡ overall spin conservation is violated.

Tables 3 and 4 summarize our measurements [14] for the reactions of C_2^- and C_2H^- with H_2, O_2, CO, CO_2, H_2O, CH_4 and C_2H_2 at 298 K. All of these reactions were observed to be slow, k_{exp} ca. $<10^{-11}$ cm^3 $mole^{-1}$ s^{-1}, with only the reaction C_2^- with O_2 having a measurable rate constant. Virtually all the channels obey spin selection rules. The failure of these reactions must, therefore, be attributed to "chemical effects" associated with constraints introduced by breaking and making of bonds required to give the products. Many of the exothermic channels in Tables 3 and 4 correspond to associative detachment of the type

$$A^- + B \rightarrow AB + e$$

which is anticipated to become generally less favourable as A and/or B become more complex. For example, in the event that the neutral is a diatomic molecule, activation energies are known [15] to arise for reactions of the "insertion" type, i.e. $A^- + BC \rightarrow BAC + e$, when the reaction exothermicity is smaller than the energy required to increase the bond distance, d_{B-C}, to its final length. Of the reaction channels in Table 3, the following clearly are of the "insertion" type whose observed non-occurrence can be rationalized in terms of the foregoing qualitative model:

$$C_2^- + H_2 \rightarrow H\text{–}C\equiv C\text{–}H + e$$
$$C_2^- + O_2 \rightarrow O\text{=}C\text{=}C\text{=}O + e$$
$$C_2^- + CO_2 \rightarrow O\text{=}C\text{=}C\text{=}C\text{=}O + e$$
$$C_2^- + CH_4 \rightarrow CH_3\text{–}C\equiv C\text{–}H + e$$
$$C_2^- + C_2H_2 \rightarrow HC\text{–}C\equiv C\text{–}CH + e$$

In some instances the insertion may be only partial, e.g.

$$C_2^- + O_2 \rightarrow O{=}C{=}O + C + e$$
$$\rightarrow O{=}C{=}O + C^-$$

or require further rearrangement, e.g.

$$C_2^- + CH_4 \rightarrow [CH_3{-}C{\equiv}C{-}H]^- \rightarrow H_2C{=}C{=}CH_2 + e$$

In all cases, however, the formation of the intermediate BAC^- probably involves an activation energy barrier. We suggest that the observed non-occurrence of some of the remaining exothermic channels for the reactions of C_2^- and C_2H^- listed may result from constraints imposed on the stereochemistry by the electrostatic interaction between the negative ion and the neutral substrate during the collision.

For example, in the reaction, $C_2^- + H_2$, the induced dipole–induced dipole interaction at small separation may result in a preferential alignment of these two species which prevents access to the free electron on the radical anion, and therefore, prevents the attachment of an H atom, e.g.

$$\overset{\delta^+\delta^-}{\cdot CC{:}^- + H{:}H} \not\rightarrow H{:}CC{:}^- + H\cdot$$

Another area of rate constant measurements in which we are currently engaged [16] concerns those ion–molecule reactions which have recently gained favour in explaining the synthesis of polyatomic molecules observed in dense interstellar clouds. Exoergic ion–molecule reactions generally have rate constants several orders of magnitude greater than those involving only neutral species and can, therefore, be effective processes at the low pressures of interstellar space. If the rate constants follow classical (ADO) behaviour they would remain effective at the low temperatures of these clouds in contrast to most two-body,molecule–molecule reactions. The ion H_3^+ is believed to be the most abundant ion in such clouds and the initiator of many of the proposed mechanisms. Since we had previously [17, 18] measured the rates of many reactions of this ion it seemed. logical to extend the measurements to other reactions proposed in the mechanisms

Take as an example, the mechanism recently proposed, independently, by Herbst and Klemperer [19] and by Watson [20] to explain the formation of HCN (or HNC). This mechanism consists of the reactions

$$NH_3^+ + H_2 \rightarrow NH_4^+ + H \quad (3)$$
$$NH_4^+ + e \rightarrow NH_3 + H \quad (4)$$
$$C^+ + NH_3 \rightarrow CNH_2^+ + H \quad (5)$$
$$CNH_2^+ + e \rightarrow CNH + H \quad (6)$$

Herbst and Klemperer [19] adopted a value of $k_3 = 1 \cdot 10^{-13}$ cm^3 molecule^{-1} s^{-1}

based on the upper limit placed on this rate constant by the failure of the Boulder group to observe the reaction. In the absence of any reported measurement, a value of $2 \cdot 10^{-9}$ cm^3 molecule^{-1} s^{-1} was adopted for k_5. Both rate constants have been measured here. A value of $k_3 = (4 \pm 2) \cdot 10^{-13}$ cm^3 molecule^{-1} s^{-1} has been obtained. The rate constant for the reaction of C^+ with NH_3 was found to be $(2.3 \pm 0.2) \cdot 10^{-9}$ cm^3 molecule^{-1} s^{-1} but the major channel (95 %) for the reaction was found to be charge exchange, so that $k_5 \simeq 1.2 \cdot 10^{-10}$ cm^3 molecule^{-1} s^{-1}.

The main sink for HCN/HNC in the mechanism is the reaction

$$C^+ + HCN \rightarrow C_2N^+ + H \qquad (7)$$

for which, again, a rate constant value of $2 \cdot 10^{-9}$ cm^3 s^{-1} was assumed. We have obtained a value of $k_7 = (4.5 \pm 0.3) \cdot 10^{-9}$ cm^3 molecule^{-1} s^{-1}. Since the production rate is some 20 times slower and the loss rate some 4 times faster than those used in the models, the mechanism appears to be inadequate in explaining the amount of HCN/HNC observed in these clouds.

THERMODYNAMICS OF ION–MOLECULE REACTIONS

As mentioned at the beginning of this paper, a major emphasis of the studies of the flowing afterglow system at York University is the thermodynamics of ion–molecule reactions from which various properties of ions and neutral molecules can be derived. These properties include proton affinities, electron affiinties, gas-phase acidities and bond dissociation energies, which will now be discussed in turn.

Proton affinities

The proton affinity PA(X) of a molecule X, at temperature T, is defined as the standard enthalpy change, ΔH_T^0 for the reaction

$$HX^+ \rightarrow H^+ + X \qquad (8)$$

The standard enthalpy change for a proton transfer reaction

$$HX^+ + Y \rightleftarrows HY^+ + X \qquad (9)$$

is, therefore, equal to the difference in proton affinities, PA(Y)−PA(X). We first recognized [18] that the flowing afterglow technique could be used to determine the preferred direction of such proton transfer reactions. This information, by itself, establishes only the sign of the standard free energy change, ΔG° for reaction (9). Standard enthalpies and free energy changes have the familiar relationship

$$\Delta G^\circ = \Delta H^\circ - T\Delta S^\circ$$

For reactions which involve only the transfer of a proton from one molecule to another the entropy change ΔS° might be expected to be small so that setting $\Delta G^\circ \simeq \Delta H^\circ$ might be a reasonable approximation. Within the validity of this approximation, which will be examined in greater detail later, the establishment of the preferred direction of reaction (9) permits the ordering of the proton affinities of any two molecules X and Y.

Any experiment designed to determine bulk thermodynamic properties of a reaction must ensure that it proceeds under conditions of thermal equilibrium. The experiments were, therefore, conducted in the presence of a sufficiently large amount of carrier gas that the reactants made more than 10^3 collisions before reacting. The neutral reactant Y was added downstream to the carrier gas which contained the protonated reactant XH^+. The observation of a rapid proton transfer reaction led to the conclusion that PA(Y) > PA(X). The failure to observe a fast reaction suggested, but did not prove, the converse. For these cases, the reaction was studied in the reverse direction, viz., X was added to buffer gas containing HY^+ ions. If rapid proton transfer was observed in this direction it was concluded that PA(X) > PA(Y). In this manner the following order of proton affinities was established $Ar < H_2 \cong O_2 < N_2 < Xe < NO < CO_2 < CH_4 < N_2O < CO$. In the original publication [18] of our results we reported $PA(H_2) > PA(O_2)$ for several interesting reasons which will be mentioned below. This technique provides a very sensitive method for determining the relative order of proton affinities among a number of molecules. For example, the proton affinities of NO, CO_2 and CH_4 are quite close together. Other techniques for determining the proton affinities of these molecules had uncertainties too large to establish their order. With the present technique this order was established without ambiguity.

We then recognized that the absolute magnitude of the proton affinity difference between 2 molecules, X and Y, could be determined by measuring the equilibrium constant for reaction (9). The equilibrium constant, K, is defined by

$$K = \frac{[YH^+][X]}{[XH^+][Y]} \qquad \text{(ii)}$$

where the square brackets denote concentrations (or more rigorously the fugacities) of the species when reaction (9) has attained chemical equilibrium. It is related to the standard free energy of the reaction by the expression:

$$\Delta G^\circ = -RT \ln K$$

The equilibrium constant can be obtained either from measurements of the ratio on the RHS of eqn. (ii) under equilibrium conditions or by measuring both forward and reverse rate constants, k_f and k_r since, for elementary reactions, $K = k_f/k_r$. We have employed both methods successfully.

Before the rate constant ratio method could be used it was necessary to

develop an analytical method for obtaining accurate rate constants from the "raw" flowing afterglow data. An expression was first derived [21] for determining k_f when the extent of reverse reaction was negligible, i.e. when the reaction was far removed from chemical equilibrium. The expression took into account, in addition to chemical reaction, the loss of XH^+ ions due to ambipolar, radial and axial diffusion as well as effects caused by the neutral gas inlet and sampling ports. Next, an expression was derived for k_f (or k_r) when appreciable back reaction was taking place, viz., with the system approaching or at equilibrium. Several simplifying assumptions had to be made, principally that diffusion and reversible two-body reactions constituted the only important loss processes for the reactants.

These analytical expressions permitted the following experimental procedures in obtaining k_f and k_r. Experiments were performed under conditions in which back reactant was not added to the reaction system and the reaction was permitted to proceed only to an extent that negligible concentrations of products were formed. Plots were obtained of the logarithm of XH^+ as a function of added Y for a known fixed reaction time, an example of which is shown in Fig. 3. The first analytical expression was used to obtain a value of k_f from such a plot. An alternate experiment, in which a fixed flow of Y was added and XH^+ determined as a function of reaction length (and, consequently, of reaction time) gave identical values for k_f.

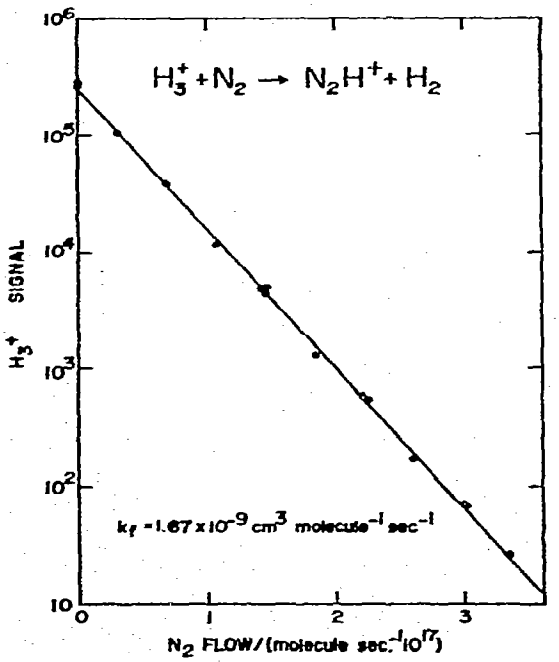

Fig. 3. A determination of the rate constant for the raction of H_3^+ with N_2 ($H_3^+ + N_2 \rightarrow N_2H^+ + H_2$), from a least squares fit to an observed decay of H_3^+ upon small additions of N_2. $T = 296$ K, $P = 0.221$ torr, $\bar{v} = 7.1 \cdot 10^3$ cm s^{-1}, $L = 81$ cm, and the flow of H_2 is $3.18 \cdot 10^{21}$ mole s^{-1}.

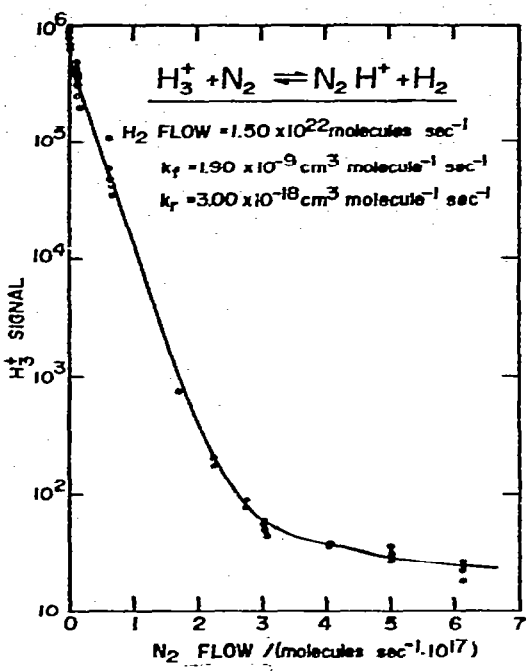

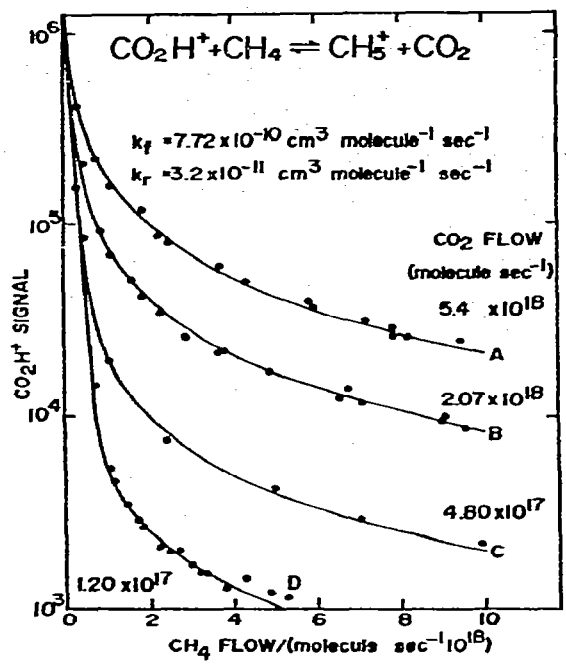

Fig. 4 (left). A determination of the rate constant for the reaction of N_2H^+ with H_2 from the best fit to an observed decay of H_3^+ upon large additions of N_2 ($H_3^+ + N_2 \rightleftarrows N_2H^+ + H_2$). The solid points represent experimental data. The solid line is a computer fit. $T = 296$ K, $P = 0.88$ torr, $\bar{v} = 8.4 \cdot 10^3$ cm s^{-1}, $L = 84$ cm, and the flow of H_2 is $1.50 \cdot 10^{22}$ molecule s^{-1}.

Fig. 5 (right). A determination of the rate constants for the reaction $CO_2H^+ + CH_4 \rightleftarrows CH_5^+ + CO_2$ from the best fits to observed decays of CO_2H^+ upon additions of CH_4 at various flows of CO_2. All four sets of data are fit using the values of k_f and k_r shown on the Fig. $T = 296$ K; $P = 0.51$ torr (for A and B), 0.419 torr (for C), 0.63 torr (for D); $\bar{v} = 8.2 \cdot 10^3$ cm s^{-1}, and $L = 59$ cm.

Experiments were then performed in which large, fixed amounts of back reactant X were added. This produced curvature in the ln XH^+ vs. Y plots as illustrated in Fig. 4. The second analytical expression was used to fit these curves to obtain k_f and k_r, and, when possible, inserting into the expression the value of k_f derived from the earlier experiments in which no back reactant is added. This method of curve fitting can provide reasonably accurate rate constant values as low as 10^{-18} cm^3 $molecule^{-1}$ s^{-1}, which is about 5 orders of magnitude lower than any previously reported rate constant from flowing afterglow experiments. When this procedure is used under conditions where the system has not attained equilibrium the ratio of the rate constants is designated $(k_f/k_r)_{ne}$. When the procedure is used under experimental conditions where chemical equilibrium is attained the ratio is designated $(k_f/k_r)_c$. In some cases, when $K \simeq 1$ and the formation of the reactant ion involves the back reactant neutral, it is not possible to obtain k_f and k_r separately, but only the ratio k_f/k_r.

Figure 5 illustrates a case for which K is closer to unity. The plots show curvature at much lower concentrations of reactant Y. The solid curves have all

been drawn with the same analytical expression, using the same values of k_f and k_r.

Equilibrium constants were also determined from the ratio of concentrations of reactants and products once chemical equilibrium has been attained. The experimental procedure can best be understood by rearranging eqn. (ii) to the form

$$\frac{[YH^+]}{[XH^+]} = K\frac{[Y]}{[X]}$$

The ratio of the ion intensities is determined as a function of Y for a fixed flow of back reactant X. If chemical equilibrium has been established a plot of the ion ratios against [Y] should produce a straight line with a slope equal to $K/[X]$. This method for obtaining K requires that the mass discrimination of the flowing afterglow system be known and techniques have been developed to determine this quantity for each equilibrium studied. On the other hand, the previous method, based on k_f/k_r ratios, does not require knowledge of the mass discrimination since it depends only on the logarithmic decrement of an ion signal.

Figure 6 demonstrates an example of an ion ratio plot for the CO_2/CH_4 system. Equilibrium is established over the entire range of Y flow rate. Figure 7 shows the plot for the N_2/H_2 system for which $K = 1.0 \cdot 10^9$. Here the plot is not linear at low flow rates of X, characteristic of conditions for which equilibrium

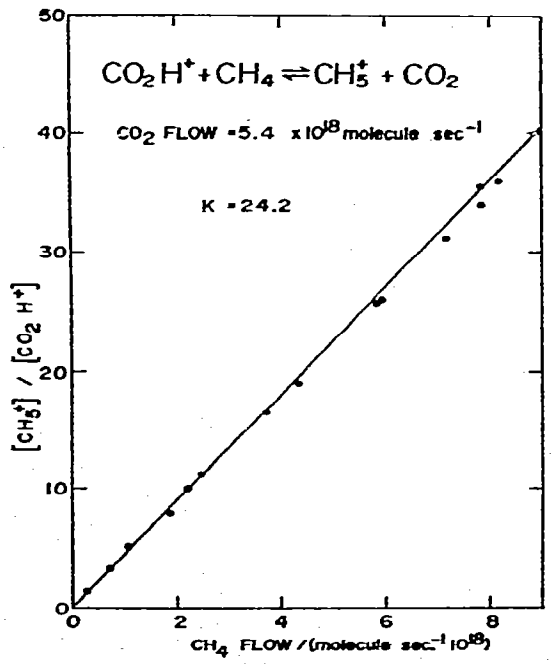

Fig. 6. The solid points represent the observed variation of $[CH_5^+]/[CO_2H^+]$ with CH_4 flow at a high flow of CO ($CO_2H^+ + CH_4 \rightleftarrows CH_5^+ + CO_2$). The solid line represents the variation computed with a value for k_f/k_r of 24.2. $T = 296$ K, $P = 0.51$ torr, $\bar{v} = 8.2 \cdot 10^3$ cm s^{-1}, and $L = 59$ cm.

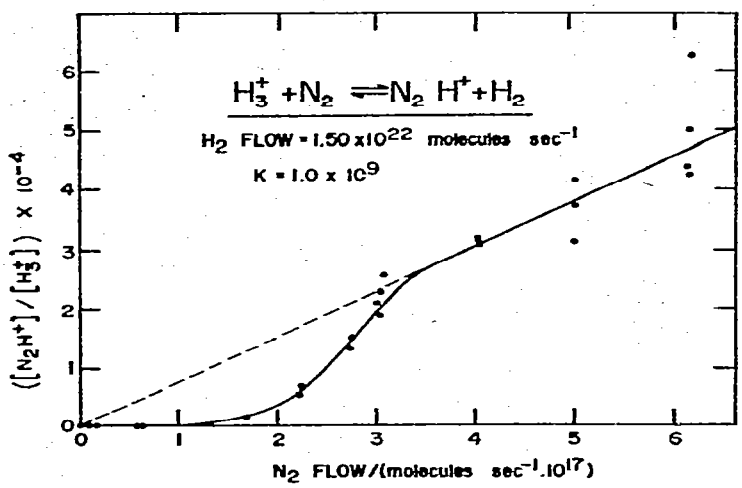

Fig. 7. The observed variation of $[N_2H^+]/[H_3^+]$ with N_3 flow showing the approach to and attainment of equilibrium, for the reaction $H_3^+ + N_2 \rightleftarrows N_2H^+ + H$. The best straight line through the data points at high N_2 flows yields a value for K of $1.0 \cdot 10^9$. $T = 296$ K, $P = 0.88$ torr, $\bar{v} = 8.4 \cdot 10^3$ cm s^{-1}, $L = 132$ cm, and the flow of H_2 is $1.50 \cdot 10^{22}$ molecules s^{-1}.

TABLE 5

FORWARD AND BACK RATE CONSTANTS, RATE CONSTANT RATIOS AND EQUILIBRIUM CONSTANT MEASUREMENTS

	$H_3^+ + N_2 \rightleftarrows N_2H^+ + H_2$	$CO_2H^+ + CH_4 \rightleftarrows CH_5^+ + CO_2$	
	Forward direction	*Forward direction*	*Reverse direction*
k_f(cm^3 $mole^{-1}$ s^{-1})	19[a] $(1.8 \pm 0.2) \cdot 10^{-9}$	13[a] $(7.8 \pm 0.2) \cdot 10^{-10}$	3[a] $(7.8 \pm 0.3) \cdot 10^{-10}$
k_r(cm^3 $mole^{-1}$ s^{-1})	4 $(5.1 \pm 2.1) \cdot 10^{-18}$	10 $(3.2 \pm 0.2) \cdot 10^{-11}$	3 $(3.3 \pm 0.1) \cdot 10^{-11}$
$(k_f/k_r)_{ne}$	4 $(4.4 \pm 1.5) \cdot 10^8$	10 24 ± 1	3 24 ± 1
$(k_f/k_r)_e$		3 24 ± 1	4 24 ± 1
K	4 $(9.3 \pm 4.0) \cdot 10^8$	4 25 ± 1	2 23 ± 1

[a] Number of experiments.

has not yet been attained. Equilibrium is approached at high flow rates of Y although there is considerable scatter in the points producing some uncertainty in the value of K. Fortunately, however, since $\Delta G°$ is proportional to the logarithm of K, it is relatively insensitive to this uncertainty.

A comparison of the values of the equilibrium constants obtained by these methods for the two systems used in the above examples is shown in Table 5. The agreement between the two independent methods, K and k_f/k_r is typical. Two other points are worth mentioning here which demonstrate the validity of these methods. The values of k_f, k_r, k_f/k_r and K were all found to be independent of reactant concentration. Agreement of $(k_f/k_r)_{ne}$ with $(k_f/k_r)_e$ and with K might be expected only if Maxwell–Boltzmann distributions hold for both reactants and products. Such a condition cannot exist immediately after the reaction has occurred.

The observation that the rate constant ratios away from equilibrium are identical to those at equilibrium indicates that sufficient non-reactive collisions occur in the flowing afterglow system to ensure that Maxwell–Boltzmann distributions are always maintained, or, less likely, that the rate constant in both directions is independent of the energy distribution.

As mentioned above, measurements of the equilibrium constant provide ΔG° for a proton transfer reaction whereas the difference between the proton affinities of X and Y is given by ΔH°. If the equilibrium constant is measured over a range of temperatures, ΔH^0 can be obtained from the van't Hoff relation $\Delta H^0 = -R\partial lnK/\partial(1/T)$. Such measurements were undertaken [22] in collaboration with the Boulder group for two typical reactions. The temperature of the Boulder flowing afterglow system can be varied over a considerable range. Figure 8 shows the ion ratio plots obtained at 4 temperatures for the reaction $CO_2H^+ + CH_4 \rightleftarrows CH_5^+ + CO_2$. The linearity of these plots shows that equilibrium was attained under all conditions depicted. Similar plots were obtained when the reaction was initiated in the reverse direction.

Figure 9 shows the van 't Hoff plots from which values of ΔH^0 and ΔS^0 were obtained from the slopes and intercepts respectively.Table 6 shows these thermodynamic quantities for this reaction and the reaction $N_2OH^+ + CO \rightleftarrows HCO^+ + N_2O$ for which equilibrium constants were also obtained in both direc-

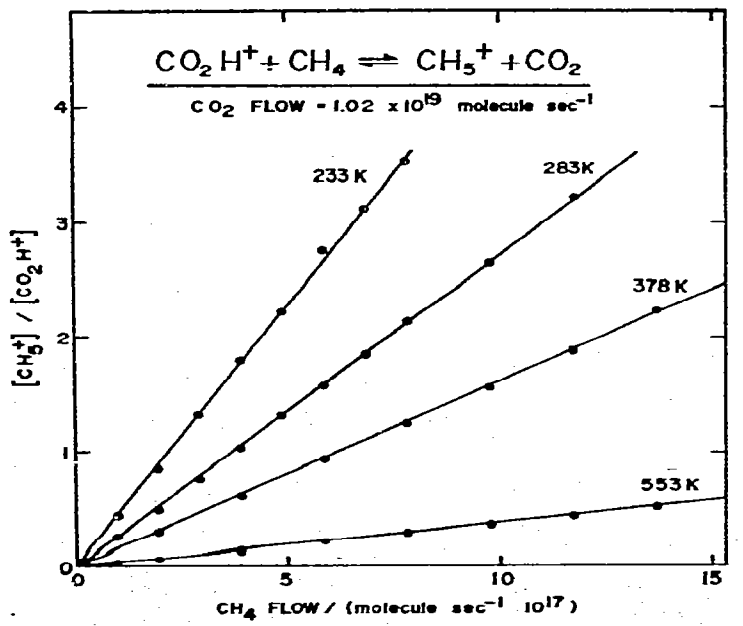

Fig. 8. The observed variation of the ratio of the product to the reactant ion signal, $[CH_5^+]/[CO_2H^+]$, with the flow of neutral reactant, CH_4, at constant flow of neutral back reactant, CO_2, at four different temperatures. The slopes of the best straight lines drawn through the points yield equilibrium constants of 46.8, 27.9, 16.4 and 6.8 at 233, 283, 378, and 553 K, respectively.

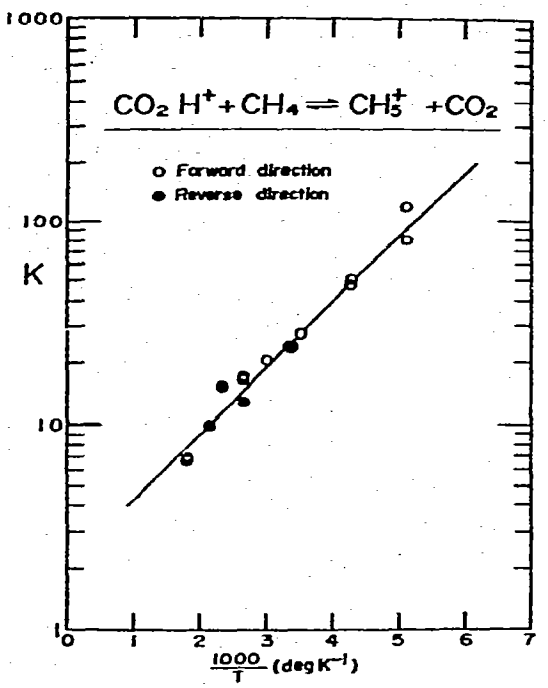

Fig. 9. A van't Hoff plot of the experimental results obtained for the proton transfer between CO_2 and CH_4 over the temperature range 196–553 K. A least squares fit to the data yields $\Delta H^\circ = -0.064 \pm 0.004$ eV from the slope and $\Delta S^\circ = +1.4 \pm 0.3$ e.u. from the intercept.

TABLE 6

KINETIC AND THERMODYNAMIC MEASUREMENTS MADE OVER A TEMPERATURE RANGE

$CO_2H^+ + CH_4 \rightleftarrows CH_5^+ + CO$
$k_f = (7.8 \pm 0.2) \cdot 10^{-10}$ cm^3 mole^{-1} s^{-1} at 296 K
$K_{296} = 24 \pm 1$
ΔH° (196–553 K) $= -0.064 \pm 0.004$ eV
ΔS° (196–553 K) $= +1.4 \pm 0.3$ e.u.
$N_2OH^+ + CO \rightleftarrows HCO^+N_2O$
$k_f = (4.95 \pm 0.07) \cdot 10^{-10}$ cm^3 mole^{-1} s^{-1} at 296 K
$K_{296} = 143 \pm 18$
ΔH° (277–505 K) $= -0.151 \pm 0.009$ eV
ΔS° (277–505 K) $= -1.8 \pm 0.7$ e.u.

tions as a function of temperature. It will be seen that ΔG^0 and ΔH^0 at 298 K differ by 0.018 and −0.023 eV for the two reactions, respectively. Thus, the assumption that $\Delta G^\circ \simeq \Delta H^\circ$ would have introduced errors in the order of 0.02 eV in the proton affinity differences.

The experimental determination of ΔS^0 for these reactions can also provide interesting information about the geometry of protonated molecules. The entropies

of the neutral species in these reactions are known. Recent ab initio calculations on the geometries of HCO^+ and CH_5^+ permit statistical thermodynamic calculations of S^0 for these ions. Combinations of these quantities with our determination of ΔS^0 yield values for S^0 (CO_2H^+) of 55.6 ± 0.6 e.u. and of S^0 (N_2OH^+) of 54.9 ± 1.1 e.u. If these ions were linear, statistical thermodynamics would give values of 52.0 e.u. and 51.9 e.u. respectively, which is lower than the experimental values by amounts greater than the estimated errors. This may be taken as evidence that the ground state geometries of these ions are not linear.

Since the temperature of our flowing afterglow system could not be varied, ΔS^0 was obtained indirectly and ΔH^0 calculated from the measured ΔG^0 values. The values of S^0 for the neutral reactants are usually well established. In many cases values for S^0 for the protonated ions have been calculated theoretically. When such theoretical values were not available, the standard entropy for the protonated ion was taken to be equal to that for its isoelectronic neutral counterpart.

Table 7 gives measured ΔG^0 values for a number of pairs of molecules, the measured or calculated values of ΔS^0, and the proton affinity differences. This Table leads to a ladder which permits proton affinity differences to be obtained between any two members.

The proton affinity difference between O_2 and H_2 is of interest for two reasons. As mentioned earlier we had originally concluded that $PA(H_2) > PA(O_2)$ on the basis of our failure to observe a large rate constant for the reaction

TABLE 7

DIFFERENCES IN THERMODYNAMIC PROPERTIES FOR PROTON TRANSFER REACTIONS OF THE TYPE $XH^+ + Y \rightleftarrows YH^+ + X$

	Measured ΔG^0_{298} (*kcal mole*$^{-1}$)	ΔS^0_{298} (*cal mole*$^{-1}$ *deg*$^{-1}$)	ΔH^0_{298} ($= \Delta P.A.$) (*eV*)	*P.A.* (*eV*)
CO				6.2[b]
	−2.9	−1.8[a]	0.15	
N_2O				6.0
	−6.2	−4[c]	0.32	
CH_4				5.7
	−1.88	+1.4[a]	0.063	
CO_2				5.6
N_2				4.9
	−12.0	−2.0[c]	0.55	
H_2				4.3[d]
	−0.03	+0.22[c]	−0.002	
O_2				4.3

[a] Measured values [22].
[b] Calculated [23].
[c] Estimated.
[d] Theoretical value [24].

TABLE 8

STANDARD HEATS OF FORMATION OF NEGATIVE IONS, STANDARD HEATS OF FORMATION[a] AND ELECTRON AFFINITIES OF CORRESPONDING RADICALS

R	$\Delta H^0_{f,298}(R^-)$	$\Delta H^0_{f,298}(R)$	$E.A.$ (R)
NH_2	25.4±0.9	40±3[a]	0.6±0.2
CH_3NH	30.5±1.4	43.6±1	0.6±0.1
C_2H_5NH	21.2±1.1	38±3	0.7±0.2
$(CH_3)_2N$	24.7±1.3	39.3±1	0.6±0.1

[a] For references to $\Delta H^0_{f,298}(R)$ see ref. 28.

$H_3^+ + O_2 \rightarrow O_2H^+ + H_2$. We now recognize that this was the result of conducting the reaction with H_2 as the carrier gas which induced a large amount of back reaction. The rate constant of this reaction was subsequently measured in a He carrier and found to be $\gg 1.3 \cdot 10^{-10}$ cm^3 s^{-1}. This reaction is also one of several observed for which ΔG^0 and ΔH^0 have opposite signs. Under these conditions a reaction may occur spontaneously (i.e. have a large k) even though it is endothermic.

It will be readily apparent that Table 7 could become a table of absolute proton affinities for each member if a value for the proton affinity of one of them were accurately known. A critical evaluation of the several possibilities for this reference value is being made, and Table 7 shows two such possibilities.

Electron affinities, acidities, and bond dissociation energies

The equilibrium studies described above have also been applied to negative ions, particularly to proton transfer reactions of the type

$$X^- + YH \rightleftarrows Y^- + XH \qquad (10)$$

By analogy to the preceding discussion of reaction (9) involving positive ions, equilibrium constant measurements of reaction (10) can provide values for the relative proton affinities, in this case of the negative ions X^- and Y^-. In addition, such measurements can also lead to values of electron affinitities and bond dissociation energies. This is illustrated in the "algorithm" shown in Fig. 10. Again, the fundamental measurement is that of the equilibrium constant, K, which provides a value for ΔG^0 for the reaction. If ΔS^0 is either measured or estimated, ΔH^0 can be obtained. The standard enthalpy change can be written in terms of the standard heats of formation, ΔH^0_f, i.e.

$$\Delta H^0 = \Delta H^0_f(Y^-) + \Delta H^0_f(XH) - \Delta H^0_f(X^-) - \Delta H^0_f(YH)$$

Obviously, a knowledge of any three of these heats of formation will permit the

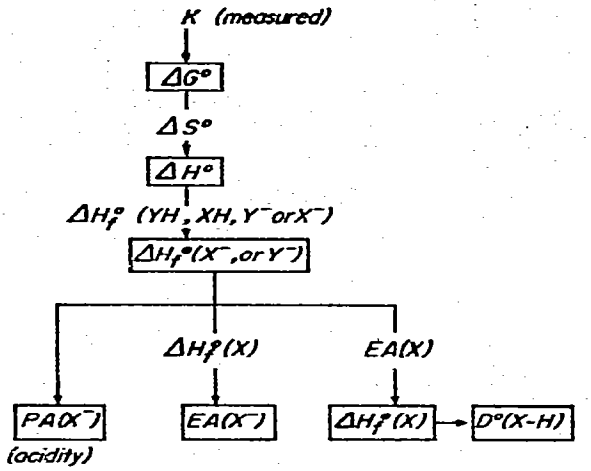

Fig. 10. Thermodynamic "algorithm" for negative ion proton transfer reactions.

evaluation of the fourth. Thus, if one knows ΔH_f^0, for XH and YH (which is frequently the case) and for one of the ions, Y^-, the heat of formation of the other ion, X^-, can be derived. Since the proton affinity of the ion is defined as ΔH^0 for the reaction

$$XH \rightarrow X^- + H^+ \tag{11}$$

and since $\Delta H_f^0(XH)$ and $\Delta H_f^0(H^+)$ are both known, this derived value of $\Delta H_f^0(X^-)$ leads directly to the proton affinity.

The electron affinity EA is defined as ΔH^0 for the process

$$X^- \rightarrow X + e \tag{12}$$

Thus, if the value of $\Delta H_f^0(X)$ is known, the derived value of $\Delta H_f^0(X^-)$ leads to EA(X).

Alternately, if the electron affinity of the radical, X, is known, combination with $\Delta H_f^0(X^-)$ leads to the heat of formation of the radical, $\Delta H_f^0(X)$, which in turn, can be combined with the heat of formation of XH to give the bond dissociation energy $D^0(H–X)$.

This general approach can be illustrated with the reaction

$$NH_2^- + H_2 \rightleftarrows H^- + NH_3 \tag{13}$$

which readily achieves equilibrium [25] at room temperature within the range of concentrations and times available in our flowing afterglow experiments. Figure 11 illustrates the rate constant ratio method and Fig. 12, the ion ratio method for determining the equilibrium constant of reaction (13). The measured equilibrium constant $K = 26 \pm 6$ corresponds to a standard free energy change $\Delta G_{298}^0 = -1.92 \pm 0.15$ kcal mole^{-1}, which leads to $\Delta H_{298}^0 = -3.20 \pm 0.30$ kcal mole^{-1} for an estimated $\Delta S_{298}^0 = -4.3 \pm 0.5$ cal mole^{-1} deg^{-1}. This value of ΔH_{298}^0,

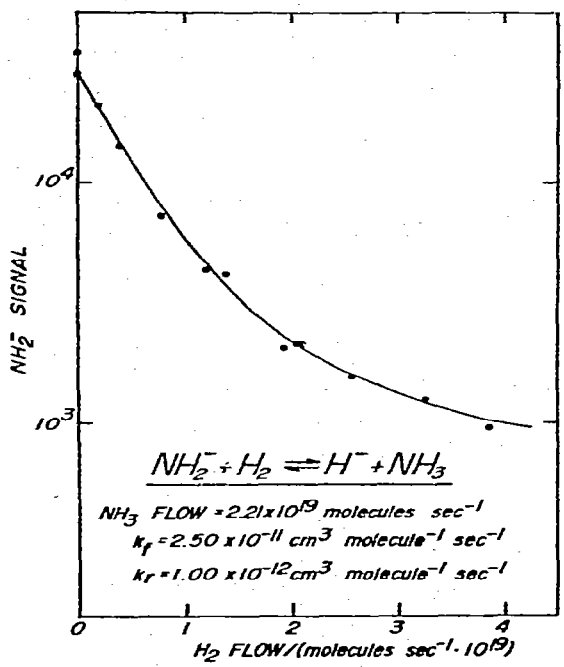

Fig. 11. A determination of the rate constants for the reaction $NH_2^- + H_2 \rightleftarrows H^- + NH_3$ from the best fit (solid line) to the observed decay (full circles) of NH_2^- upon addition of H_2 at a fixed flow of NH_3. $T = 298$ K, $P = 0.409$ torr, $\bar{v} = 8.5 \cdot 10^3$ cm s^{-1} and $L = 60$ cm.

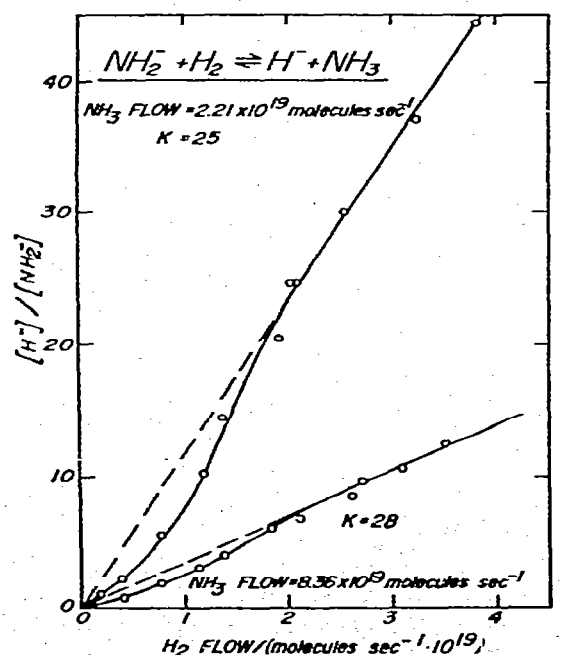

Fig. 12. The approach to and attainment of equilibrium as manifested by the observed variation of the ratio of the product to the reactant ion signal $[H^-]/[NH_2^-]$, with flow of neutral reactant, H_2, at two different flows of back-reactant, NH_3. $T = 298$ K, $P = 0.409$ torr, $\bar{v} = 8.5 \cdot 10^3$ cm s^{-1}, and $L = 60$ cm. The equilibrium constants are determined from the slopes of the best straight lines through the open circles at high flows of H_2.

when combined with established values of $\Delta H^0_{f,298}$ for H^- and NH_3, leads to $\Delta H^0_{f,298}(NH_2^-) = 25.4 \pm 0.9$ kcal mole^{-1}. From the definition given above the proton affinity $PA(NH_2^-) = 403.6 \pm 0.5$ kcal mole^{-1}.

The available literature values of $\Delta H^0_f(NH_2)$ can be combined with our determination of $\Delta H^0_f(NH_2^-)$ to obtain a value of the electron affinity $EA(NH_2) = 14.7 \pm 4$ kcal mole^{-1} $= 0.64 \pm 0.17$ eV which compares favourably with the recent determinations by Smyth and Brauman [26] of 0.744 ± 0.022 eV and of Cellotto et al. [27] of 0.779 ± 0.037 eV. Both these determinations involve photodetachment by laser light and, therefore, provide values of ΔH^0_0 for process (12) rather than ΔH^0_{298} evaluated in our method.

Actually, the photodetachment values are much more reliable than the value of $\Delta H^0_f(NH_2)$ used in our calculation. In this case, therefore, it is more productive to combine the photodetachment value for $EA(NH_2)$ with our value of $\Delta H^0_f(NH_2^-)$ to obtain a value for $\Delta H^0_{f,298}(NH_2)$ of 44.3 ± 1.1 kcal mole^{-1}, which can then be combined with the established value of $\Delta H^0_{f,298}(NH_3)$ to give $D^0_{298}(NH_2\text{–}H) = 107.4 \pm 1.1$ kcal mole^{-1}. This probably represents the most reliable value of the bond dissociation energy of NH_3 available to date.

We have now extended our efforts to determine thermochemical parameters for negative ions to simple aliphatic amines and alcohols, methyl cyanide, acetylene, allene and ketene [28]. Table 8 summarizes heats of formation and electron affinities determined from the measurement of equilibrium constants for reactions of the type

$$NH_2^- + R_1R_2NH \rightleftarrows R_1R_2N^- + NH_3$$

$$H^- + R_1R_2NH \rightleftarrows R_1R_2N^- + H_2$$

where R_1 and R_2 may be H, CH_3 or C_2H_5.

The values for the standard free energy changes, ΔG^0_{298} which can be determined from the equilibrium constants, provide a measure of the relative intrinsic (gas phase) acidity of the Bronsted acids XH and YH. Reference to well established acidities of H, and/or H_2O can then lead to a scale of intrinsic acidity as shown in Fig. 13. Here acidity is defined as the standard free energy change for process (11). Such information can begin to allow a quantitative assessment of the influence of intrinsic molecular properties which is often dominated in solution by environmental solvent effects.

Although many of these studies of equilibrium constants have involved proton transfer to negative ions and neutral molecules we hasten to point out that the methods discussed above are quite general and could be applied equally well to other reactions such as charge transfer, S_N2 reactions, and atom–ion interchange, to name only a few examples.

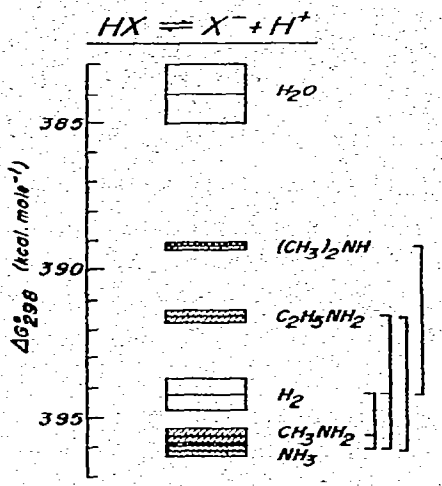

Fig. 13. Scale of intrinsic acidities. The measured relative acidities of pairs of Bronsted acids are represented by the brackets shown on the right hand side of the figure. The scale is set by the well established value of the acidity of H_2. The width of the bars represent the experimental uncertainty.

ACKNOWLEDGEMENTS

We wish to express our appreciation for the collaboration of our co-workers A. E. Roache, R. S. Hemsworth, H. W. Rundle, G. I. Mackay, P. R. Fennelly, J. D. Payzant and D. Betowski.

REFERENCES

1 E. E. Ferguson, F. C. Fehsenfeld and A. L. Schmeltekopf, *Advan. At. Mol. Phys.*, 5 (1969) 1.
2 T. Su and M. T. Bowers, *J. Chem. Phys.*, 58 (1973) 3027.
3 G. Gioumousis and D. P. Stevenson, *J. Chem. Phys.*, 29 (1958) 294.
4 T. F. Moran and W. H. Hamill, *J. Chem. Phys.*, 39 (1963) 1413.
5 S. K. Gupta, E. G. Jones, A. G. Harrison and J. J. Myer, *Can. J. Chem.*, 45 (1967) 3107.
6 T. Su and M. T. Bowers, *Int. J. Mass Spectrom. Ion Phys.*, 12 (1973) 347.
7 R. S. Hemsworth, J. D. Payzant, H. I. Schiff and D. K. Bohme, *Chem. Phys. Lett.*, 26 (1974) 417.
8 P. J. Kuntz and A. C. Roach, *Trans. Faraday Soc.*, 11 (1972) 259.
9 A. Dedieu and A. Veillard, *J. Amer. Chem. Soc.*, 94 (1972) 6730.
10 P. F. Fennelly, J. D. Payzant, R. S. Hemsworth and D. K. Bohme, *J. Chem. Phys.*, 60 (1974) 5115.
11 D. K. Bohme, G. I. Mackay and J. D. Payzant, *J. Amer. Chem. Soc.*, 96 (1974) 4027.
12 L. B. Young, E. Lee-Ruff and D. K. Bohme, *Chem. Comm.*, 35 (1973).
13 H. F. Calcote, in J. L. Franklin (Ed.), *Ion–Molecule Reactions*, Vol. 2, Plenum Press, New York, 1972, Ch. 15.
14 H. I. Schiff and D. K. Bohme, unpublished results.
15 F. C. Fehsenfeld and E. E. Ferguson, *J. Chem. Phys.*, 51 (1969) 3512.
16 H. I. Schiff, R. S. Hemsworth, J. D. Payzant and D. K. Bohme, *Ap. J.*, 191 (1974) 49.
17 J. A. Burt, J. L. Dunn, M. J. McEwan, M. M. Sutton, A. E. Roche and H. I. Schiff, *J. Chem. Phys.*, 52 (1970) 6062.
18 A. E. Roche, M. M. Sutton, D. K. Bohme and H. I. Schiff, *J. Chem. Phys.*, 55 (1971) 5480.

19 E. Herbst and W. Klemperer, *Ap. J.*, 185 (1973) 505.
20 W. D. Watson, *Ap. J.*, 188 (1973) 35.
21 D. K. Bohme, R. S. Hemsworth, H. W. Rundle and H. I. Schiff, *J. Chem. Phys.*, 58 (1973) 3504.
22 R. S. Hemsworth, H. W. Rundle, D. K. Bohme, H. I. Schiff, D. B. Dunkin and F. C. Fehsenfeld, *J. Chem. Phys.*, 59 (1973) 61.
23 C. S. Matthews and P. Warneck, *J. Chem. Phys.*, 51 (1969) 854.
24 A. J. Duben and J. L. Lowe, *J. Chem. Phys.*, 55 (1971) 4270.
25 D. K. Bohme, R. S. Hemsworth and H. W. Rundle, *J. Chem. Phys.*, 59 (1973) 77.
26 K. C. Smyth and J. I. Brauman, *J. Chem. Phys.*, 56 (1972) 4620.
27 R. J. Celotta, R. A. Bennett and J. L. Hall, *J. Chem. Phys.*, 60 (1974) 1740.
28 G. I. Mackay, R. S. Hemsworth, H. I. Schiff and D. K. Bohme, *J. Amer. Chem. Soc.*, to be submitted.